Astron. Astrophys. 213, 411–422 (1989)

ASTRONOMY AND ASTROPHYSICS

The stability of nonlinear dynamos and the limited role of kinematic growth rates

A. Brandenburg[1], **F. Krause**[2], **R. Meinel**[2], **D. Moss**[3] **and I. Tuominen**[1]

[1] Observatory and Astrophysics Laboratory, University of Helsinki, Tähtitorninmäki, SF-00130 Helsinki, Finland
[2] Sternwarte Babelsberg, Akademie der Wissenschaften der DDR, Rosa-Luxemburg-Str. 17a, DDR-1591 Potsdam, German Democratic Republic
[3] Department of Mathematics, The University, Manchester M13 9PL, England

Received July 22, accepted September 1, 1988

Summary. The physical significance of growth rates of kinematic dynamos is discussed in the context of the observation that usually a magnetic field of a single symmetry dominates in the Sun and other cosmic objects. It is concluded that these growth rates are not the decisive factor determining the final state of the field. The possibility that the stability of different solutions of nonlinear dynamos determines the final state is investigated with the help of several models. The examples of simple α^2-dynamos investigated show that, in spite of the asymptotic equality of the kinematic growth rates, usually the only solution which remains stable is that with the smallest marginal dynamo number. Dynamo models in spherical geometry are found, however, in which both symmetric and antisymmetric solutions are stable. The kind of symmetry finally established depends in these cases on the initial conditions, i.e. on the history of the object. In no case was a steady solution found that was a superposition of the two distinct symmetry types, that is a non-symmetric steady final state was never reached. However, in connection with the investigations of the oscillatory dynamo we discovered a case where both the symmetric and the antisymmetric solutions are unstable. The attractor is in this case a torus: non-symmetric quasiperiodic solutions oscillate between the unstable symmetric and antisymmetric solutions with a long period.

Key words: hydromagnetic dynamos – nonlinear stability – the Sun: magnetic field

1. Introduction

The typical astrophysical dynamo is modelled by an electrically conducting rotating sphere, the internal structure and the motions of which show symmetry with respect to the rotational axis and to the equatorial plane. In the kinematic case a model of that kind excites eigenmodes of different symmetry types. The fields will either show symmetry or antisymmetry with respect to the equatorial plane. We denote them by S and A, and will also speak about even (S) and odd (A) modes.

The essence of kinematic mean-field dynamos may be found in stability maps, which display the lines of zero growth rates for the different eigenmodes $\boldsymbol{B}_n$. An example is given in Fig. 1. C_α and C_ω are dimensionless parameters characterizing the α-effect and differential rotation. In the denotation Am and Sm, the number m corresponds to the dependence on the longitude by $e^{im\phi}$.

Clearly, one wishes to know which of these eigenmodes will be realised for the cosmic object considered. Obviously this depends where the object is situated in that diagram. In region (i), where only one mode has a positive growth rate, a unique answer can be given: a field of type $A0$ will be excited. In region (ii) a field of type $S0$ has also a positive growth rate and will compete with the $A0$-field. Region (iii) represents a much more complicated, already highly nonlinear, situation where non-axisymmetric modes will also grow.

It is widely assumed that in the competition between different $\boldsymbol{B}$-modes the one with the largest growth rate wins. In this way a criterion seems to exist and may be checked by observation. However, calculations of growth rates carried out earlier (Yoshimura et al., 1984) have revealed that a significant difference between the growth rates of fields with different parity exists only close to the critical dynamo number. All numerical examples studied so far show that the growth rates of the first odd parity mode and the first even one are asymptotically equal for large dynamo numbers. In this way practically no decision is possible unless one assumes that the dynamo number of the cosmic object, e.g. the Sun, is close to the critical value.

We investigate here the behaviour of the growth rates of further models. First we consider dynamo models in which this problem can be treated analytically. Then we calculate numerically solar-type $\alpha\omega$-dynamos. In all cases we will find the growth rates of the first modes of even and odd parity are asymptotically equal.

The observational results from the Sun and the planets Earth, Jupiter, and Saturn reveal that these objects excite magnetic fields with a clear dominance of one parity, in these cases the odd one. In the Sun this is most clearly manifested by Hale's polarity law revealing the dominance of the odd parity for the toroidal field. Stenflo and Vogel (1986) furthermore derived the result that only the odd parity of the poloidal field has a clear 22-year cycle.

Consequently we have to conclude that the criterion based on the growth rates does not apply. A quite different criterion was formulated by Krause and Meinel (1988), who postulated that the stability of nonlinear solutions determines which field is finally excited by an object. We follow here this approach and

Send offprint requests to: F. Krause

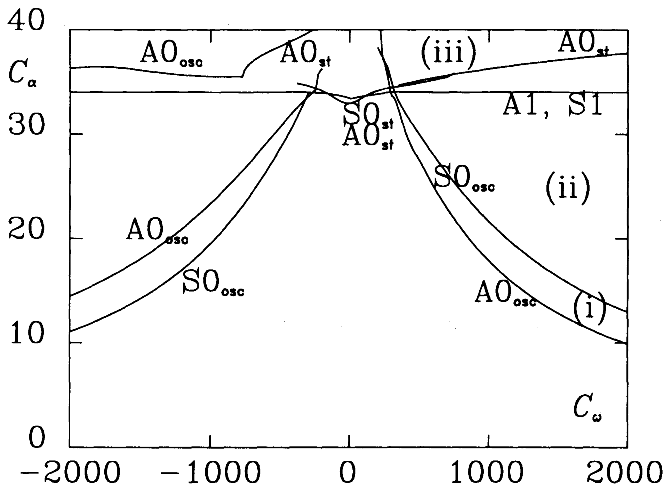

Fig. 1. A stability map for the kinematic dynamo model of Steenbeck and Krause (1969). The lines of zero growth rate are plotted for different modes A0, S0, A1 and S1 in $C_\alpha - C_\omega$-plane. The subscripts "st" and "osc" refer to stationary and oscillatory modes. The sign of C_ω is such that on the right hand side ($C_\omega > 0$) the angular velocity ω is increasing inwards from the surface of the sphere. The regions (i), (ii), and (iii) represent different degrees of nonlinearity (see text)

study the nonlinear behaviour of a one-dimensional α^2-model and furthermore investigate numerically certain nonlinear α^2- and $\alpha\omega$-models in spherical geometry.

2. A spherical dynamo with α = const.

As shown by Krause and Steenbeck (1967), the spherical α^2-dynamo with α = const. may be represented in terms of Bessel functions whose order is half an odd integer. The growth rate λ_{nl} of the mode $\boldsymbol{B}_{nl}$ is determined by the set of equations

$$\lambda_{nl} = u_{nl}^{(1)} \cdot u_{nl}^{(2)}, \tag{1}$$

$$C_\alpha = u_{nl}^{(1)} + u_{nl}^{(2)}, \tag{2}$$

and

$$J_{n+1/2}(u_{nl}^{(1)}) J_{n-1/2}(u_{nl}^{(2)}) - J_{n-1/2}(u_{nl}^{(1)}) J_{n+1/2}(u_{nl}^{(2)}) = 0, \tag{3}$$

with $u_{nl}^{(1)} \neq u_{nl}^{(2)}$. $C_\alpha = \mu\sigma\alpha R$ is the dynamo number, where μ is the magnetic permeability, σ the conductivity and R the radius of the sphere. n denotes the order of the multipole, which is the form of $\boldsymbol{B}_{nl}$ outside of the sphere. l denotes the number of knots inside of the sphere in the radial direction (Krause and Rädler, 1980, Sect. 14.4).

We consider the case where C_α is large and fixed. Then the largest value of λ_{nl} is given by that pair of $u_{nl}^{(1)}$, $u_{nl}^{(2)}$ which satisfies (3) and for which $u_{nl}^{(1)} \approx u_{nl}^{(2)} \approx C_\alpha/2$. Let $u_{nl}^{(i)} = C_\alpha/2 + \delta_i$, $i = 1, 2$. From (2) it follows that

$$\delta_1 + \delta_2 = 0. \tag{4}$$

Using the asymptotic representation of Bessel functions we find from (3)

$$\delta_1 = l\pi/2[1 + 2n/C_\alpha^2(n + (-1)^{n+1}\cos C_\alpha)] + O(C_\alpha^{-3}), \tag{5}$$

and from (1)

$$\lambda_{nl} = (C_\alpha^2 - l^2\pi^2)/4 - l^2\pi^2 n/C_\alpha^2 \times [n + (-1)^{n+1}\cos C_\alpha] + O(C_\alpha^{-3}). \tag{6}$$

We see that, indeed, for all modes the growth rates have an asymptote which is independent of the order of the multipole n. The asymptote depends on the number l of knots in the radial direction only.

3. A one-dimensional α^2-model

We will consider now the basic equations

$$\partial\boldsymbol{B}/\partial t = \operatorname{curl}(\alpha\boldsymbol{B}) + (\mu\sigma)^{-1}\Delta\boldsymbol{B} \tag{7}$$

inside a plane layer ($-d \leq z \leq d$);

$$\operatorname{curl}\boldsymbol{B} = 0 \tag{8}$$

outside the layer ($|z| > d$); and

$$\operatorname{div}\boldsymbol{B} = 0 \tag{9}$$

everywhere. $\boldsymbol{B}$ is continuous at the boundaries of the layer and vanishes as $|z| \to \infty$. We seek solutions of the form $\boldsymbol{B} = \boldsymbol{B}(z, t)$. This leads to the equations

$$\begin{aligned} \partial B_x/\partial t &= -\partial(\alpha B_y)/\partial z + (\mu\sigma)^{-1}\partial^2 B_x/\partial z^2 \\ \partial B_y/\partial t &= \partial(\alpha B_x)/\partial z + (\mu\sigma)^{-1}\partial^2 B_y/\partial z^2 \end{aligned} \tag{10}$$

for the nonvanishing components $B_x(z, t)$ and $B_y(z, t)$, with the boundary conditions

$$B_x(d, t) = B_y(d, t) = B_x(-d, t) = B_y(-d, t) = 0. \tag{11}$$

We note that Eqs. (10) and (11), with B_x and B_y replaced by B_r and B_ϕ, are often used as a simple model to study axisymmetric disk dynamos within the "local approximation" (cf. Zeldovich et al., 1983). However, this approximation is not well justified, as mentioned by Rädler and Bräuer (1987). In particular the use of the boundary condition (11) is not correct in that context. We therefore consider the model (10), (11) only as a mathematical idealization (one-dimensional reduction) of the 3-dimensional α^2-dynamo problem.

Introducing dimensionless coordinates ζ, τ, defined by

$$t = \mu\sigma d^2\tau, \qquad z = d\zeta, \tag{12}$$

and the complex function

$$B(\zeta, \tau) = B_x + iB_y, \tag{13}$$

we obtain the equation

$$\dot{B} = B'' + iC_\alpha(\tilde{\alpha} f B)', \qquad C_\alpha = \mu\sigma\alpha_0 d, \tag{14}$$

with the boundary conditions

$$B(1, \tau) = B(-1, \tau) = 0. \tag{15}$$

Here we have assumed

$$\alpha = \alpha_0\tilde{\alpha}(z) f(BB^*) \tag{16}$$

where α_0 is a positive constant, $\tilde{\alpha}(z)$ a prescribed function of z and $f(BB^*)$ a prescribed function modelling the back-reaction of the magnetic field on the turbulence.

Now we consider the special case

$$\tilde{\alpha} = \begin{cases} \ \ 1 & \text{for } 0 < \zeta < 1 \\ -1 & \text{for } -1 < \zeta < 0 \end{cases} \tag{17}$$

and discuss first the kinematic problem, i.e. $f \equiv 1$. The general solution of the problem (14), (15), (17) is given by

$$B = B^{(A)} + B^{(S)}, \tag{18}$$

where

$$B^{(A)}(-\zeta,\tau) = -B^{(A)}(\zeta,\tau),$$
$$B^{(S)}(-\zeta,\tau) = B^{(S)}(\zeta,\tau). \tag{19}$$

$B^{(A)}$ and $B^{(S)}$ are solutions of (14) for $0 \le \zeta \le 1$ with the boundary conditions

$$B^{(A)}(0,\tau) = 0, \quad B^{(A)}(1,\tau) = 0, \tag{20}$$

$$B^{(S)\prime}(0,\tau) + iC_\alpha B^{(S)}(0,\tau) = 0, \quad B^{(S)}(1,\tau) = 0. \tag{21}$$

The conditions at $\zeta = 0$ follow from the continuity of B and $B' + iC_\alpha \tilde{\alpha} B$ (see Eq. (14)) together with Eq. (19). These solutions can be found in the form

$$B^{(A)} = \sum_{n=1}^{\infty} c_n^{(A)} e^{\lambda_n^{(A)}\tau} B_n^{(A)}(\zeta), \tag{22}$$

$$B^{(S)} = \sum_{n=1}^{\infty} c_n^{(S)} e^{\lambda_n^{(S)}\tau} B_n^{(S)}(\zeta), \tag{23}$$

where $c_n^{(A)}$ and $c_n^{(S)}$ are arbitrary complex constants determined by the initial conditions.

The antisymmetric modes (for $0 \le \zeta \le 1$) are given by

$$B_n^{(A)}(\zeta) = e^{-iC_\alpha\zeta/2} \sin n\pi\zeta \tag{24}$$

with the eigenvalues

$$\lambda_n^{(A)} = C_\alpha^2/4 - n^2\pi^2. \tag{25}$$

The symmetric modes are ($0 \le \zeta \le 1$)

$$B_n^{(S)}(\zeta) = e^{-iC_\alpha\zeta/2} \sin[\delta_n(1-\zeta)] \tag{26}$$

with the eigenvalues

$$\lambda_n^{(S)} = C_\alpha^2/4 - \delta_n^2, \tag{27}$$

where the δ_n have to be determined as nontrivial solutions of the transcendental equation

$$\delta_n = \frac{i}{2} C_\alpha \tan\delta_n. \tag{28}$$

Without loss of generality we assume $\mathrm{Re}\,\delta_n > 0$, and arrange the solutions according to

$$(2n-1)\pi/2 < \mathrm{Re}\,\delta_n < n\pi.$$

In contrast to the antisymmetric modes, the symmetric modes have always complex eigenvalues $\lambda_n^{(S)}$. The growth rates $\mathrm{Re}\,\lambda_n$ for the first modes are depicted in Fig. 2. The first S-mode is growing for $C_\alpha > 4.0066$, the first A-mode for $C_\alpha > 2\pi$. For large C_α the growth rates become undistinguishable. This can also be seen by comparing the asymptotic expansion of (27), (28)

$$\lambda_n^{(S)} = C_\alpha^2/4 - n^2\pi^2 + 4in^2\pi^2/C_\alpha + 12n^2\pi^2/C_\alpha^2 + O(C_\alpha^{-3}) \tag{29}$$

with (25), i.e.

$$\mathrm{Re}\,\lambda_n^{(S)} - \mathrm{Re}\,\lambda_n^{(A)} = 12n^2\pi^2/C_\alpha^2 + O(C_\alpha^{-3}). \tag{30}$$

Thus the results of the kinematic analysis can be symmarized as follows: For $C_\alpha < 4.0066$ no dynamo activity is possible, any initial magnetic field will decay. For $4.0066 < C_\alpha < 2\pi$ a symmetric magnetic field mode will grow. For $C_\alpha > 2\pi$ symmetric and antisymmetric modes are growing and a prediction of the final state is impossible on the basis of the kinematic results alone.

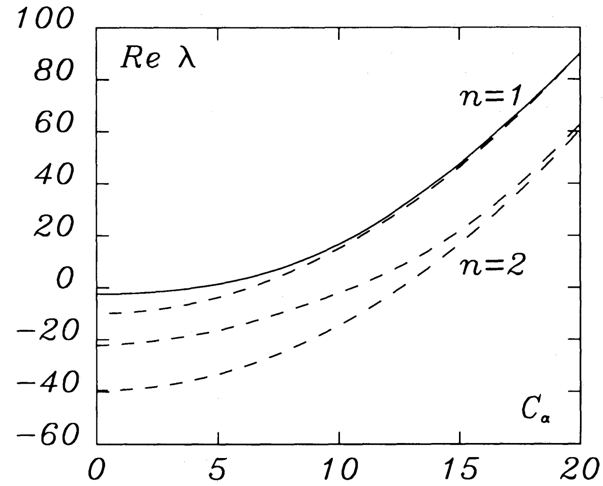

Fig. 2. Growth rates of different modes in the one-dimensional α^2-model. The solid curve denotes the growth rate $\lambda_1^{(S)}$ of the first symmetric mode and dashed ones refer to the next higher A- and S-modes. Note the convergence of modes with the same n, but different symmetry

4. Growth rates for αω-dynamos of solar type

In this section we present results of numerical calculations concerning the growth rates of some $\alpha\omega$-dynamos. We will find further evidence that the asymptotic equality will also hold here, although a rigorous proof is not available.

First we investigate the growth rate of the first odd parity mode and the first even mode for the Steenbeck–Krause model 1 (Steenbeck and Krause, 1969). The results are given in Table 1. λ denotes the growth rate and Ω_m the frequency of the magnetic cycle. Both quantities are here dependent only on the dynamo number $C_\alpha C_\omega$, where C_α is determined as before and C_ω is a dimensionless measure of the differential rotation. We find that the magnetic field $B \equiv 0$ becomes unstable for $C_\alpha C_\omega \approx 20.7\,10^3$ and here a field of type $A0$ with a dipole parallel to the axis of

Table 1. The frequency and growth rate for model 1 of Steenbeck and Krause (1969) for different values of the dynamo number $C_\alpha C_\omega$. These eigenvalues in this and the other tables were computed with 100 radial gridpoints and 14 spherical harmonics

	A0 mode		S0 mode	
$10^{-3}C_\alpha C_\omega$	$\pm\Omega_m$	λ	$\pm\Omega_m$	λ
0.	.0	-9.9	.0	-20.2
10.	22.2	-8.0	20.4	-17.1
20.	31.2	-0.4	29.6	-6.3
30.	37.9	5.9	36.5	1.3
40.	43.2	11.3	42.1	7.5
50.	47.8	16.2	46.9	12.8
60.	51.9	20.6	51.2	17.5
80.	59.1	28.3	58.6	25.7
100.	65.4	35.1	65.2	32.8

Table 2. The frequency and growth rate for different values of C_α for the same model as in Table 1, but the α-effect producing the toroidal field from the poloidal one is included. $C_\omega = 1000$. See also Fig. 1 and Fig. 3

	A0 mode		S0 mode	
C_α	$\pm\Omega_m$	λ	$\pm\Omega_m$	λ
0.	.0	-9.9	.0	-20.2
10.	22.3	-7.6	20.3	-16.0
20.	31.6	2.1	29.9	-2.1
30.	37.8	13.3	36.5	11.5
40.	39.1	26.3	37.8	26.1
50.	41.0	35.8	39.8	35.8

rotation will start to grow. From $C_\alpha C_\omega \approx 28.3\,10^3$ on, a field of type $S0$ will also grow, but the growth rate of the $A0$-type field remains larger.

When the α-effect producing the toroidal field from the poloidal one is not neglected compared with effects of differential rotation, the asymptotic equality of $A0$ and $S0$ modes is more clearly demonstrated. This can be seen from Table 2 and Fig. 3, where we present the results for this case using model 1 of Steenbeck and Krause with $C_\omega = +1000$. The growth rates of the two fields become undistinguishable for $C_\alpha > 40$. The results for a further model with α and ω profiles as in Rädler (1986, Fig. 16) are presented in Table 3 and Fig. 4. The behaviour of the growth rates is here more complicated. For example the growth rates of the S-type solution exceed that of the antisymmetric one for certain C_α values. For even higher C_α the $S0$-mode splits into two non-oscillatory solutions. This does *not* mean that a new eigenvalue emerged because all axisymmetric oscillatory modes have a pair of complex conjugated eigenvalues. Also the $A0$-solution becomes non-oscillatory, but the second eigenvalue

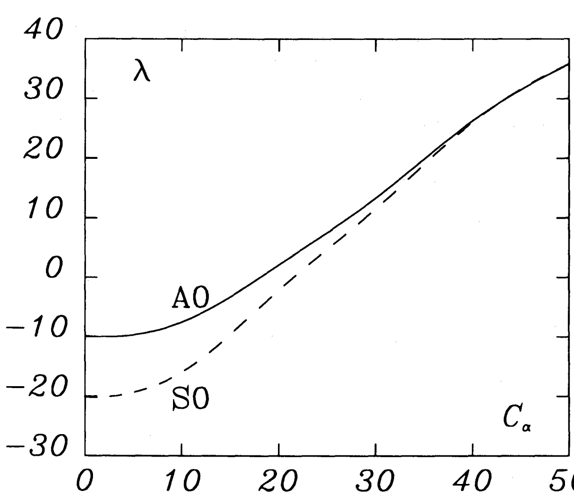

Fig. 3. Growth rates of the first A- and S-type solutions (solid and broken lines, respectively) for the same model as in Fig. 1 for $C_\omega = +1000$. The α-effect producing the toroidal field from the poloidal one is not neglected here, in contrast to the model used in Table 1

Table 3a. The frequency and growth rate for different C_α of a model with α and ω profiles as in Rädler (1986, Fig. 16) with $C_\omega = -1000$. See also Fig. 4. For $C_\alpha > 3.2$ the first modes are only non-oscillatory and their growth rates become asymptotically equal

	A0 mode				S0 mode			
	1. mode		2. mode		1. mode		2. mode	
C_α	$\pm\Omega_m$	λ	$\pm\Omega_m$	λ	$\pm\Omega_m$	λ	$\pm\Omega_m$	λ
.0	.0	-9.9			.0	-20.2		
0.1	.0	-14.1			.0	-13.6		
0.5	11.9	-11.5			.0	-8.2		
1.0	15.7	-7.5			.0	-5.2		
1.5	17.7	-4.1			.0	-3.7		
2.0	18.8	-0.5			2.5	-6.7		
2.2	18.9	1.1			6.4	-3.9		
2.4	18.8	2.9			8.4	-0.8		
2.6	18.1	4.9			9.6	3.0		
2.8	16.7	7.1			9.9	7.2		
3.0	13.1	9.2			8.6	12.3		
3.05	11.7	9.4			8.0	13.4		
3.10	8.8	9.0	.0	-10.2	6.9	14.9		
3.15	.0	13.6	7.6	1.4	4.7	16.6		
3.20	.0	20.3	11.6	1.5	.0	19.1	.0	17.4
3.25	.0	25.1	13.4	2.3	.0	25.0	.0	14.4
3.30	.0	29.4	14.3	3.2	.0	29.4	.0	13.4
3.40	.0	37.6	15.0	5.2	.0	37.7	.0	12.6
3.50	.0	45.9	14.6	7.2	.0	46.0	.0	12.3
3.60	.0	54.6	13.0	9.3	.0	54.6	.0	11.7
3.70	.0	63.8	9.4	11.2	.0	63.8	.0	14.8
3.80	.0	73.5	.0	20.0	.0	73.5	.0	23.7
4.00	.0	94.5	.0	40.2	.0	94.5	.0	40.6

Table 3b. The frequency and growth rate of the first non-axisymmetric modes A1 and S1 for some values of C_α using the same model as in Table 3a. Note that the growth rates of both symmetries are always very close to each other

	A1 mode		S1 mode	
C_α	Ω_m	λ	Ω_m	λ
2.0	995.2	-22.0	1000.4	-21.4
2.6	997.9	-8.7	999.3	-8.5
2.8	999.6	-1.0	999.1	-1.0
3.0	999.0	8.5	999.2	8.6
3.2	999.4	19.8		

transforms with another non-oscillatory one to a pair of complex conjugate oscillatory modes.

All these calculations have in common the asymptotic equality of the growth rates for $A0$ and $S0$ modes. This result was also obtained by Yoshimura et al. (1984) for different types of models. We further see that there also seems to be asymptotic equality for

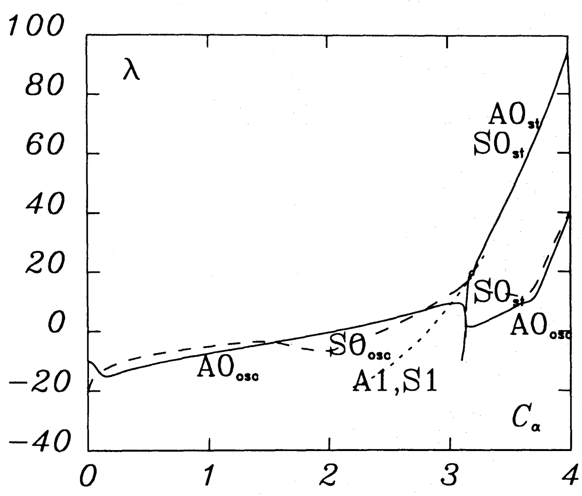

Fig. 4. Growth rates of the first A- and S-type solutions for a model with α and Ω profiles as in Rädler (1986, Fig. 16). We have chosen $C_\omega = -1000$, which means that Ω increases inwards with his definition. Note that the growth rates of the S-type solution (dotted) exceeds that of the antisymmetric one (solid) for C_α between 2.8 and 3.2. For even higher C_α and S0 branch splits into two non-oscillatory modes. The A0-solution becomes also non-oscillatory, but the second eigenvalue transforms with another non-oscillatory one to a pair of complex conjugate oscillatory modes

the fields of type $S1$ and $A1$, although with an asymptote which differs from that of $A0$ and $S0$ (see Table 3b). These numerical results confirm the conjecture that no decision between odd and even parity fields can be based on the considerations of the growth rates of the linear eigenmodes.

5. Nonlinear analysis of the one-dimensional α^2-model

The dynamo model treated in Sect. 3 allows the reduction of the solution of the nonlinear steady problem to a quadrature. It can easily be shown that antisymmetric steady nonlinear solutions are possible. The boundary conditions (20) reduce the problem for $(0 \le \zeta \le 1)$ to the model discussed by Krause and Meinel (1988). While symmetric steady solutions are impossible, solutions of the form

$$B^{(S)}(\zeta, \tau) = \tilde{B}(\zeta) e^{i\Omega_m \tau} \tag{31}$$

can be found, where Ω_m is a real constant to be determined as the eigenvalue of the ordinary differential equation

$$i\Omega_m \tilde{B} = \tilde{B}'' + iC_\alpha [f(\tilde{B}\tilde{B}^*)\tilde{B}]' \tag{32}$$

following from (14) for $0 \le \zeta \le 1$. The corresponding boundary conditions are

$$\begin{aligned} &\tilde{B}' + iC_\alpha f(\tilde{B}\tilde{B}^*)\tilde{B}|_{\zeta=0} = 0, \\ &\tilde{B}(1) = 0. \end{aligned} \tag{33}$$

The steady nonlinear solutions of A-type bifurcate from the trivial solution $B \equiv 0$ at the critical values $C_{\alpha n}^{(A)} = 2n\pi$ and coincide there with the steady kinematic modes. Correspondingly the symmetric solutions (31) bifurcate at the marginal values $C_{\alpha n}^{(S)}$ of the symmetric oscillatory kinematic modes. At $C_{\alpha n}^{(S)}$ the eigenvalues Ω_{mn} of (32), (33) coincide with $\mathrm{Im}\,\lambda_n^{(S)}$.

We considered more closely the case

$$f(BB^*) = 1/(1 + BB^*). \tag{34}$$

Numerical stability tests of the different nonlinear solutions have been carried out using (14) for $-1 \le \zeta \le 1$ without symmetry restrictions. The first S-type solutions (bifurcating at $C_{\alpha 1}^{(S)} = 4.0066$, see Fig. 5a) proves to be stable against arbitrary perturbations. The first A-type solution (bifurcating at $C_{\alpha 1}^{(A)} = 2\pi$) is stable against antisymmetric perturbations but unstable against symmetric perturbations. All higher solutions of both types are unstable.

A particular stability test was based on the quantity P defined by

$$P = [E^{(S)} - E^{(A)}]/[E^{(S)} + E^{(A)}], \tag{35}$$

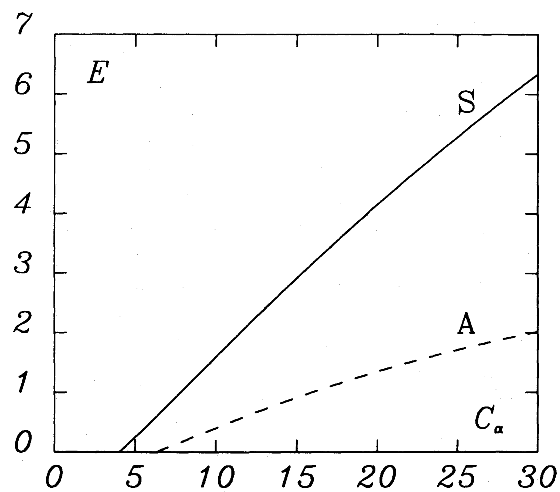

Fig. 5a. Bifurcation diagram for the nonlinear one-dimensional α^2-model. The S-type solution is oscillatory and the frequencies deviate quite substantially from those of the linear theory, if C_α is large. The energy for the oscillatory solution is time independent

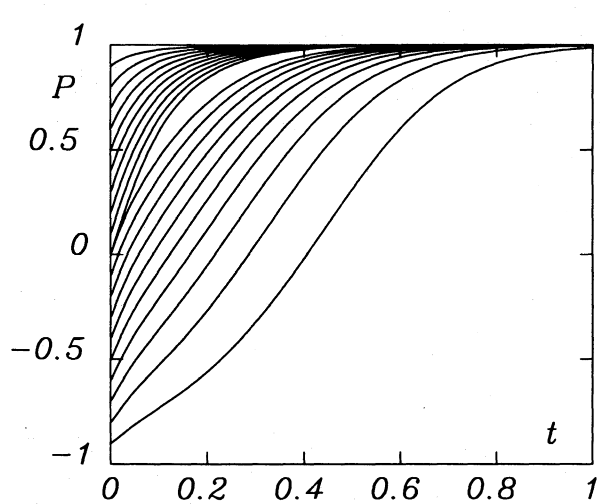

Fig. 5b. Evolution of P for the one-dimensional α^2-model of Fig. 5a. For all different initial ε (or P) the solution turns into a pure symmetric one, i.e. $P = 1$. These curves were obtained by taking $C_\alpha = 8$

where $E^{(S)}$ and $E^{(A)}$ are the energies of the symmetric and antisymmetric part of the $\boldsymbol{B}$-field inside the conducting region. Note that $P=1$ for a pure symmetric field and $P=-1$ for a pure antisymmetric one. The energy is defined here as

$$E^{(S/A)} = 1/2 \int_{\text{volume}} d^3x\,|\boldsymbol{B}^{(S/A)}|^2 \tag{36}$$

where $\boldsymbol{B}^{(S)}$ and $\boldsymbol{B}^{(A)}$ denote the symmetric and antisymmetric part of $\boldsymbol{B}$.

We now test the stability of the A-type solution by adding a fraction ε of the S-type solution to the $\boldsymbol{B}$-field:

$$\boldsymbol{B}_0 = \boldsymbol{B}^{(A)} + \varepsilon \boldsymbol{B}^{(S)}. \tag{37}$$

Similarly the stability of the S-type solution is tested by taking

$$\boldsymbol{B}_0 = \boldsymbol{B}^{(S)} + \varepsilon \boldsymbol{B}^{(A)} \tag{38}$$

as the initial condition.

Figure 5b gives the evolution of P in the one-dimensional model for different initial disturbances obtained by step by step integration of B in time for initial values of P in the range $(-1, +1)$. Note that we used (37) for $P<0$ and (38) for $P>0$, and moreover that the initial condition is not fixed by P alone but also by relative phase of $B^{(A)}$ and $B^{(S)}$. However, the qualitative nature of the results is not affected by this freedom of initial conditions. We find that the final stable solution has the value $P=1$, i.e. the parity is symmetric. Our investigations show that the final state resulting from any initial field (except from the unrealistic situation of a *pure* antisymmetric initial field without any symmetric part) will always be given by the first S-type nonlinear solution. This solution can be considered as the nonlinear extension of the first marginal S-mode. We stress that this result of the clear prevalence of the S-type solution has nothing to do with the different kinematic growth rates.

6. Nonlinear dynamo models in spherical geometry

Analytical solutions for dynamo models in spherical geometry with latitudinally dependent α are not available. We shall therefore study the stability of such models numerically, restricting ourselves, however, to the axisymmetric case. We solve the dynamo equations (7)–(9) on a two-dimensional grid employing a DuFort–Frankel time advance (see Proctor, 1977). When the calculation is performed in two quadrants of a meridional plane of a sphere, the boundary conditions do not select the parity, and fields of both parities can exist simultaneously.

6.1. Dependence of α on the total energy

We now make a special choice of nonlinearity, where α depends on the total magnetic energy $E = E^{(S)} + E^{(A)}$ (the "cross term" vanishes under the integral):

$$\alpha = \alpha(\theta) = C_\alpha \cos\theta/(1+E). \tag{39}$$

C_α is the dynamo number and α is independent of r and changes sign at the equator. The bifurcation of the S- and A-type solutions from the trivial one appears at the critical dynamo numbers $C_\alpha^{(S)} = 7.81$ and $C_\alpha^{(A)} = 7.64$. These are in accordance with those calculated for the same model by Roberts (1972). For $C_\alpha > C_\alpha^{(S/A)}$, $|\boldsymbol{B}|$ and so E grow until the quantity $C_\alpha/(1+E)$ is reduced to the critical value, $C_\alpha^{(S/A)}$, of the currently dominant mode. Then the steady state is reached. The energies are therefore determined by:

$$E^{(S/A)} = C_\alpha / C_\alpha^{(S/A)} - 1. \tag{40}$$

The stability behaviour can readily be observed by following the time evolution of P, defined in Eq. (35). In Fig. 6a we have plotted the energy versus dynamo number for solutions of each parity.

In Fig. 6b we have plotted P versus time for different ε such that the initial P again covers the range from -1 to $+1$. Clearly the A-type solution is stable to symmetric disturbances and the S-type solution unstable to antisymmetric disturbances. This is further illustrated by an experiment in which the evolution of a purely S-type initial field was followed over many diffusion times. The field evolved to the steady S-type solution ($P=+1$) in time $t=O(1)$ with $C_\alpha/(1+E) = C_\alpha^{(S)}$, and this configuration persisted until $t \gg 1$. Finally however this S-type solution changed

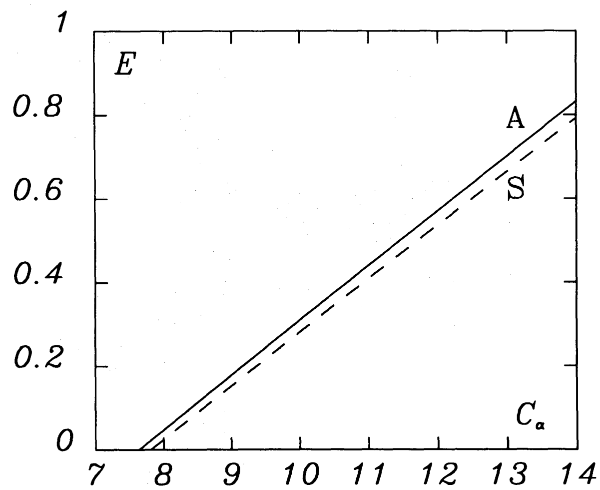

Fig. 6a. Bifurcation diagram for a spherical dynamo model with α depending on the total energy E only (see Eq. (39)). The energy increases linearly with C_α

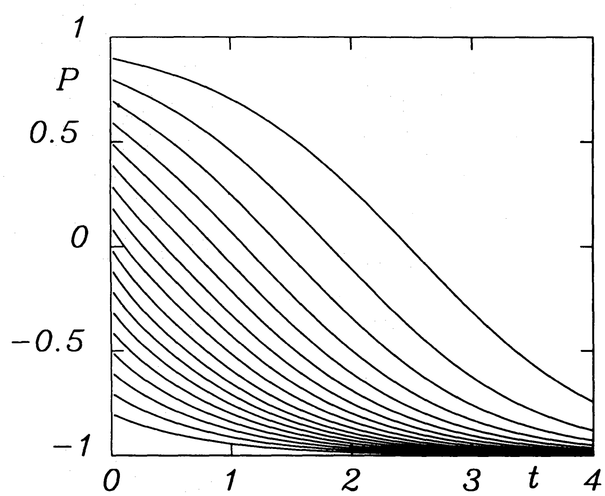

Fig. 6b. Evolution of P for the spherical dynamo model of Fig. 6a. For all different initial ε (or P) the solution turns into a pure antisymmetric one, i.e. $P=-1$. These result was obtained using $C_\alpha = 10$

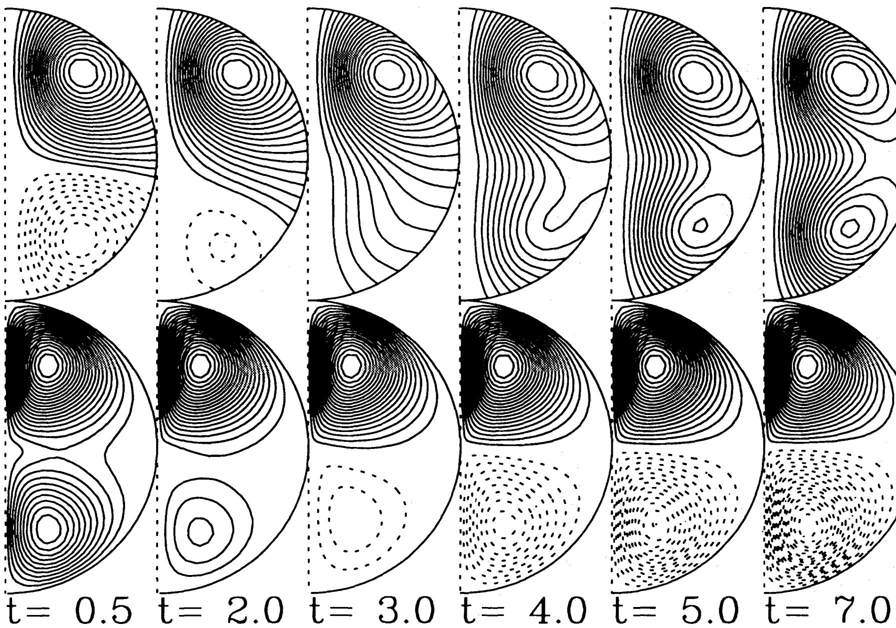

Fig. 7. Series of snapshots showing the change of symmetry for a nonlinear dynamo, where α depends only on the total energy. (Field lines of the poloidal field above and lines of constant field strength of the toroidal field below) The initial field consist of a symmetric field with the energy $E^{(S)} = 0.28$ disturbed by a small antisymmetric field with the energy $\varepsilon E^{(A)} = 0.015$, so that $P = 0.9$ for the initial condition. This state is unstable and evolves then to a pure antisymmetric configuration

into the first A-type solution ($P = -1$), as the A-type noise inevitably present in the computed solution grew and eventually reduced $C_\alpha/(1+E)$ to $C_\alpha^{(A)} < C_\alpha^{(S)}$. This is in agreement with the general result of Krause and Meinel (1988, Sect. 5). Note again that the mechanism is not just that of the solution with the fastest linear theory growth rate becoming exponentially larger than any other. The simple nonlinearity introduced quenches the symmetric solution by reducing an initially supercritical value of C_α to a value at which the symmetric solution decays and the antisymmetric solution is stable.

The typical time for the parity of the field to change can be estimated by means of the kinematic growth rates. A small initial antisymmetric contribution in a nearly symmetric field will increase with the growth rate $\lambda^{(A)}$. The effective α corresponds to the marginal value of the currently dominating parity, which is here the symmetric one with $C_\alpha^{(S)} = 7.81$. From linear theory we obtained for this value C_α the growth rate of the antisymmetric parity

$$\lambda^{(A)} = +0.55, \text{ when } C_\alpha = C_\alpha^{(S)}. \tag{41}$$

For a given ratio of the initial energy of the antisymmetric disturbance $E_0^{(A)}$ and the final one $E^{(A)}$ we expect the typical timescale to be

$$\tau = [2\lambda^{(A)}]^{-1} \ln [E^{(A)}/E_0^{(A)}]. \tag{42}$$

From Eqs. (35) and (40) we obtain

$$\frac{E^{(A)}}{E_0^{(A)}} = \frac{1+P}{1-P} \frac{C_\alpha/C_\alpha^{(A)} - 1}{C_\alpha/C_\alpha^{(S)} - 1}. \tag{43}$$

Considering now the uppermost curve in Fig. 6b, which starts from $P = 0.9$, we find from Eqs. (41)–(43) $\tau \approx 2.6$, which is indeed in accordance with Fig. 6b and with the series of snapshots in Fig. 7.

6.2. Dependence of α on the local energy density

The back-reaction of the magnetic field on the turbulence will in general reduce the α-effect depending on the local strength of the field, rather than on the global energy, as assumed in the previous section. In order to keep α positive, we adopt here the frequently used expression

$$\alpha = \alpha(r, \theta) = C_\alpha \cos\theta / [1 + \boldsymbol{B}(r, \theta)^2]. \tag{44}$$

We have computed solutions for different dynamo numbers (see the bifurcation diagram in Fig. 8a) and have tested their stability in the same manner as described in the previous section. The evolution of the parity after disturbances with different ε is plotted in Fig. 8b for $C_\alpha = 10$. We see that, in contrast to the previous case, there are now two stable solutions, one symmetric ($P = 1$) and the other antisymmetric ($P = -1$). Which of the possible solutions is realized depends on the initial condition. Similar results have been already obtained by Rädler (1984). From Fig. 8b it can be estimated that the "watershed" lies at

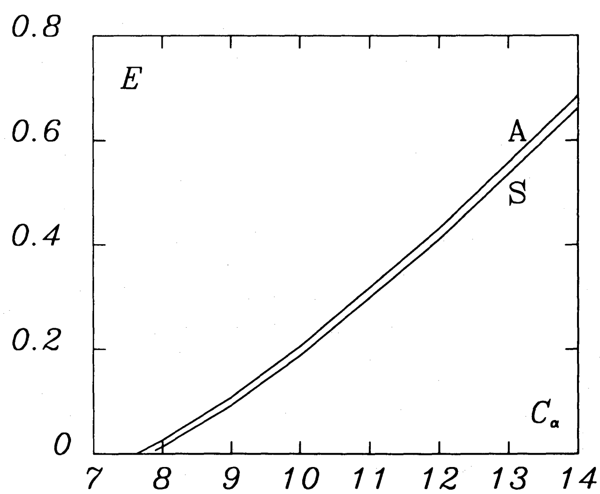

Fig. 8a. Bifurcation diagram for a spherical dynamo model with α depending on the *local* energy density $1/2\,\boldsymbol{B}^2$ (see Eq. (44)). The energy of the S-type solution remains below that of the A-type solution

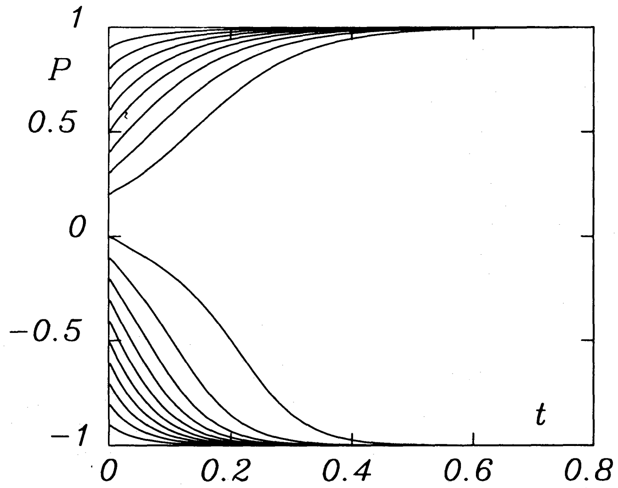

Fig. 8b. Evolution of P for the spherical dynamo model of Fig. 8a with $C_\alpha = 10$. For an initial condition with dominating symmetric parity $P > 0$ the solution reverted to a pure symmetric mode with $P = +1$, and vice versa

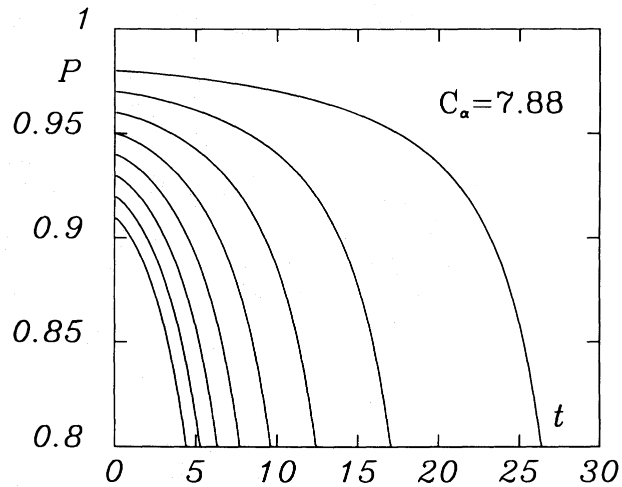

Fig. 8d. Same as Fig. 8a, but $C_\alpha = 7.88$. For all initial conditions the final solution is the antisymmetric one ($P = -1$)

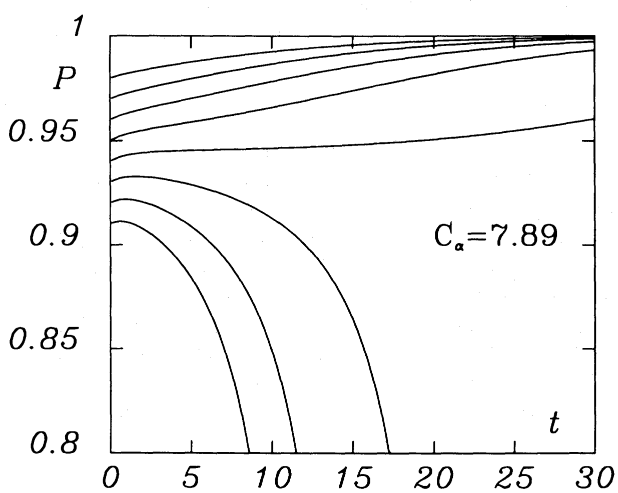

Fig. 8c. Same as Fig. 8a, but $C_\alpha = 7.89$. Only for initial conditions close to $P = 1$ the solution tends to the symmetric field

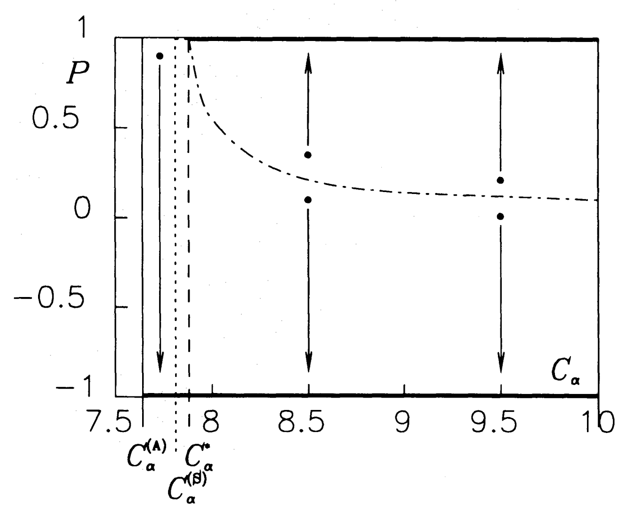

Fig. 8e. A sketch illustrating the time behaviour of the magnetic fields starting from asymmetric initial conditions ($-1 < P < +1$). $C_\alpha^{(A)}$ is the critical dynamo number. First an antisymmetric solution ($P = -1$) is attractor. Beyond $C_\alpha^{(S)}$ also a symmetric solution ($P = +1$) exists but is first unstable, the antisymmetric one is still attractor. From C_α^* onwards this symmetric solution is also stable with, as indicated by the "watershed" (dot-dash line), an increasing region of attraction

$P \approx +0.05$. This result is surprising, since the marginal dynamo numbers of both symmetries are well separated.

At first this result seems to be in contradiction to the general statement of Krause and Meinel (1988) that the second nonlinear solution, bifurcating from $C_\alpha^{(S)}$ is in any case unstable. In their denotation $C_\alpha^{(A)}$ has to be identified with C_1 and $C_\alpha^{(S)}$ with C_2. However, according to their statement the unstable behaviour necessarily appears in a certain neighbourhood of $C_\alpha^{(S)}$ only, i.e. there may exist a certain value $C_\alpha^* > C_\alpha^{(S)}$ with the property that the symmetric solution is unstable for $C_\alpha < C_\alpha^*$, but stable for $C_\alpha > C_\alpha^*$.

In order to confirm this statement we calculated the stability for values of C_α closer to $C_\alpha^{(S)}$. It is found that the "watershed" tends, indeed, to $P = 1$ if C_α tends to $C_\alpha^{(S)}$. For $C_\alpha = 7.89$ the "watershed" is very close to $P = 1$ (Fig. 8c) and for $C_\alpha = 7.88$ no stable symmetric solution was found (Fig. 8d). Hence, the results can be expressed by an inequality:

$$7.81 = C_\alpha^{(S)} < 7.88 < C_\alpha^* < 7.89. \tag{45}$$

The situation is illustrated in Fig. 8e.

We will now discuss how far we can understand the stability behaviour. If $\boldsymbol{B} = \boldsymbol{B}^{(S/A)} + \boldsymbol{b}$ is substituted in the governing equation we find by linearising with respect to the perturbation $\boldsymbol{b}$ the equation:

$$\partial \boldsymbol{b}/\partial t = \operatorname{curl}\{\alpha[r, \theta, (\boldsymbol{B}^{(S/A)})^2]\boldsymbol{b}\} + (\mu\sigma)^{-1}\Delta \boldsymbol{b} + \operatorname{curl}\left\{\left.\frac{\partial \alpha}{\partial \boldsymbol{B}^2}\right|_{\boldsymbol{B} = \boldsymbol{B}^{(S/A)}} \cdot [2\mathrm{B}^{(S/A)}\boldsymbol{b}]\boldsymbol{B}^{(S/A)}\right\}. \tag{46}$$

Where it not for the last term, the stability could be discussed in terms of the growth rates derived from the kinematic dynamo equation with modified α. Then stability of the symmetric solution $\boldsymbol{B}^{(S)}$ would be plausible if the maximal growth rate of antisymmetric modes were still negative:

$$\lambda^{(A)} < 0, \quad \text{when } \alpha = \alpha^{(S)} = \alpha(r, \theta, \boldsymbol{B}^{(S)^2}). \tag{47}$$

In the example considered above this was, however, *not* the case. For instance, we found for $C_\alpha = 10$:

$$\lambda^{(A)} = 0.62, \quad \text{when } \alpha = \alpha^{(S)} \tag{48}$$

which would be large enough for the antisymmetric solution to become important within the timespan plotted in Fig. 8b. Obviously, the influence of the last term of the righthand side of Eq. (46) provides an additional mechanism to stabilize the symmetric parity solution. The sequence of snapshots in Fig. 7 (where α is given by Eq. (39)) gives some insight into the process of partity reversal. There is a stage with very little magnetic induction in one hemisphere. Now, if the α-feedback is θ-dependent, the local α in this hemisphere will be close to the maximal possible value α_0. This leads again to a field amplification in this region. The direction of this field is still the same as before. The θ-dependent feedback is thus acting against a reversal of parity and is stabilizing the symmetric solution.

The stability of the antisymmetric solution could simply be explained by a condition similar to Eq. (47)

$$\lambda^{(S)} < 0, \quad \text{when } \alpha = \alpha^{(A)}. \tag{49}$$

In the example considered above ($C_\alpha = 10$) we indeed found:

$$\lambda^{(S)} = -0.70, \quad \text{when } \alpha = \alpha^{(A)}. \tag{50}$$

That means, the last term in Eq. (46) does not qualitatively change the stability behaviour of the antisymmetric solution.

6.3. *Feedback on the mean velocity field*

In the former sections we considered the back-reaction of the magnetic field on the turbulent motions, which reduces the α-effect. There may be, however, also a considerable feedback on the mean velocity field $\boldsymbol{u}$, which can limit the magnetic energy. Such dynamos have been investigated by Proctor (1977), who computed strictly antisymmetric dynamos. We shall study here the stability of both symmetric and antisymmetric solutions. We restrict ourselves again to the axisymmetric case and assume density ρ, kinematic viscosity ν and magnetic diffusivity η to be constant in a sphere of radius $\boldsymbol{R}$.

The governing equations are now the induction and momentum equations, which we solve simultaneously including the mean motion in the induction equation:

$$\partial \boldsymbol{B}/\partial t = \operatorname{curl}[\boldsymbol{u} \times \boldsymbol{B} + \alpha \boldsymbol{B} - \eta \operatorname{curl} \boldsymbol{B}]$$

$$\operatorname{div} \boldsymbol{B} = 0. \tag{51}$$

The momentum and continuity equations are:

$$\rho D\boldsymbol{u}/Dt = -\nabla p - 2\rho \boldsymbol{\Omega} \times \boldsymbol{u} + \rho \boldsymbol{g}_{\text{eff}} - \boldsymbol{B} \times \operatorname{curl} \boldsymbol{B}/\mu + \rho\nu\nabla^2 \boldsymbol{u},$$

$$\operatorname{div} \boldsymbol{u} = 0, \tag{52}$$

where $\boldsymbol{u}$ is the motion induced by the Lorentz force, p is pressure, $\boldsymbol{\Omega}$ the (constant) angular velocity, and $\boldsymbol{g}_{\text{eff}}$ the effective gravity. We eliminate pressure and gravity by taking the curl of the meridional part of the momentum equation. The obtained equations were solved using step by step integration in time on a two-dimensional grid with the same finite-difference representation for the nonlinear terms as Proctor. We keep the Ekman number $\nu/\Omega R^2$ and the magnetic Prandtl number ν/η equal to unity and take $\alpha = C_\alpha \cos\theta$, with C_α constant. For the velocity we employed a stress-free boundary condition at the surface of the sphere.

In Fig. 9a we have plotted a bifurcation diagram for the magnetic energies of both parities. The critical values for C_α are, of course, the same as in Sect. 6.1. We compared the energy of the A-type solution with the values given by Proctor and found good agreement.

We again studied the stability of these solutions by following the evolution of P for different disturbances. The results, which

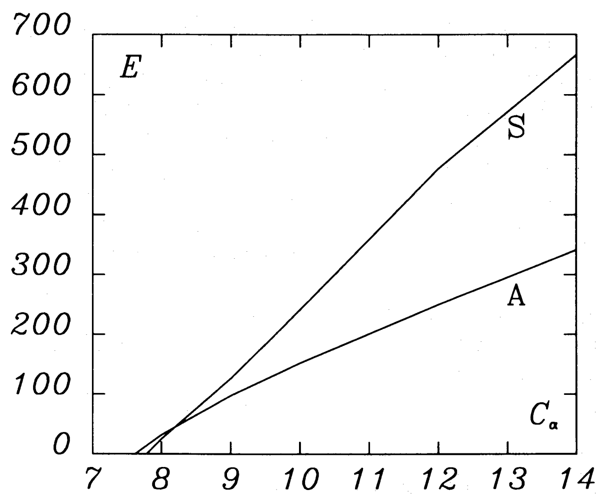

Fig. 9a. Bifurcation diagram for the spherical magneto-hydrodynamic dynamo model of Sect. 6.3, where the equations for the mean velocity are solved simultaneously with the induction equations. Note that the energy of the S-type solution exceeds that of the A-type solution for $C_\alpha > 8.2$. Such a crossing of energies was not found for the dynamo models in which the nonlinearity came only via α

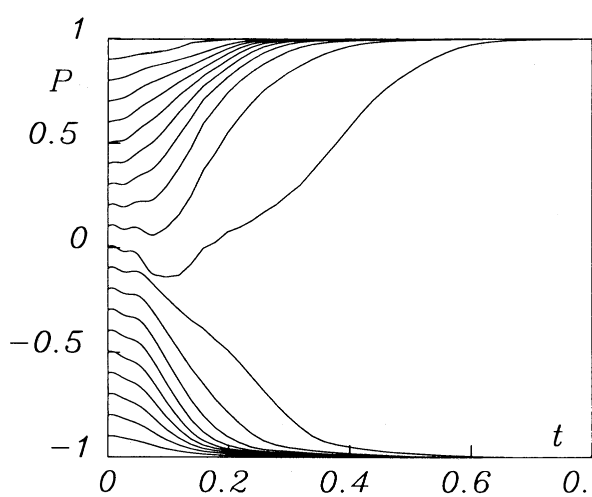

Fig. 9b. Evolution of P for the spherical magneto-hydrodynamic dynamo model of Fig. 9a. Similarly to the former case (Fig. 8b), the initial condition determines the final symmetry. $C_\alpha = 10.0$

are presented in Fig. 9b, are.similar to the case where the α-effect depends on the *local* energy density (Sect. 6.2), i.e. symmetric and antisymmetric solutions are each possible stable solutions. According to Lenz's rule we would also expect similar results to those obtained previously, since the main effect of this feedback is a *local* braking of the initially rigid rotation, creating thereby differential rotation, which gives rise to magnetic induction acting against the original field. This is inevitably a more or less dramatic simplification of a complicated physical system, whose complexity is likely to increase towards the highly nonlinear low viscosity regime.

6.4. *Nonlinear oscillatory dynamos*

In the last two sections we have considered two different nonlinear dynamo problems and found in each case conditions under which two solutions exists. This result is in contrast to those in Sects. 5 and 6.1, where only one solution was found to be stable. We argued then that the θ-dependent feedback of the α-effect may stabilize the $S0$-mode. This possible explanation could break down, however, if the magnetic field is oscillating, since the feedback (together with the local energy density) can become rather small during the cycle. This is also the case in the one-dimensional α^2-model of Sect. 5, for which only one stable solution was found. In this section we follow this point in more detail.

Oscillatory solutions of the dynamo equations in spherical geometry are known, if differential rotation is present ($\alpha\omega$-dynamo). We have studied the simple nonlinear model defined by Eq. (4)) with an angular velocity Ω varying linearly with radius:

$$\Omega(r) = C_\omega/(\mu\sigma R^2)\cdot r/R. \tag{53}$$

Keeping $C_\omega = -10^4 = \text{const}$, we found Hopf bifurcations from the trivial solution at the values $C_\alpha^{(A)} = 0.549$ and $C_\alpha^{(S)} = 0.728$ with the frequencies $\Omega_m^{(A)} = \pm 54.1$ and $\Omega_m^{(S)} = \pm 67.5$. These eigenvalues are again in accordance with those calculated by Roberts (1972) for the same model.

The stability of these two solutions of the nonlinear problem is examined by following the evolution of P for different initial conditions and values of C_α. A surprising new situation in comparison with the foregoing models appears: For $C_\alpha = 0.75$ the antisymmetric solution proves to be stable (Fig. 10a). However, for $C_\alpha = 0.9$ our calculations reveal that neither of the two nonlinear solutions is stable (Fig. 10b, c). The time behaviour of P exhibits a long period, which is about ten times the basic magnetic period. Within this long period, obviously, the magnetic field switches from a dominant symmetric state ($P > 0$) to a state where the antisymmetric part is dominating ($P < 0$) and vice versa. The trajectory in phase space of the system lies on a torus (Brandenburg et al., 1989). Then, for $C_\alpha = 1.0$ the symmetric

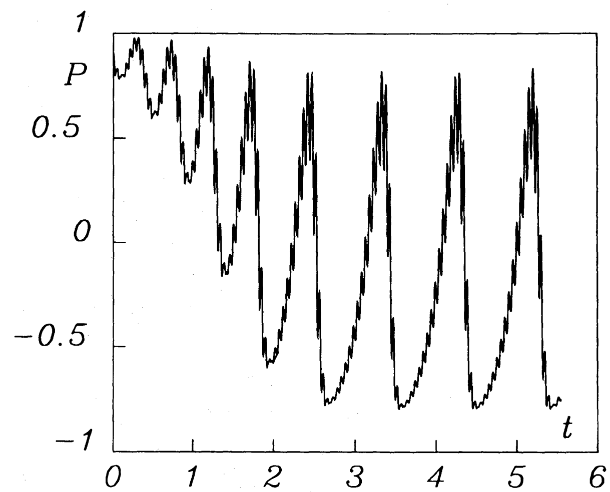

Fig. 10b. Same as Fig. 10a, but with $C_\alpha = 0.9$. Now the antisymmetric solution is also unstable. The attractor is more complex: it shows in the extreme cases either dominant symmetry or antisymmetry. The long period of this parity variation is about ten times the basic magnetic period. Note that the high frequency wiggles are due to the energy, which oscillates with half the magnetic period

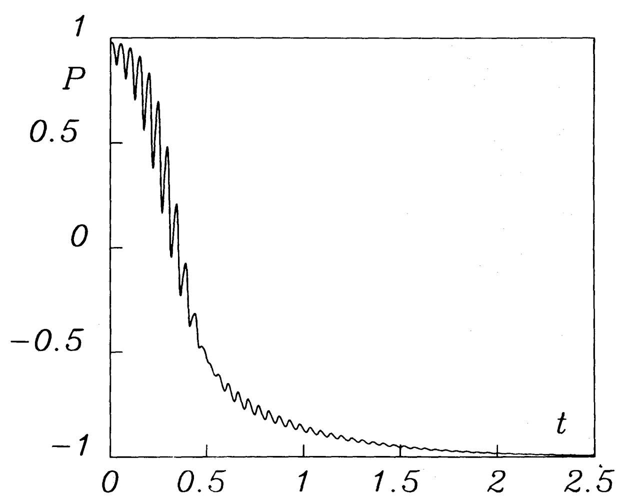

Fig. 10a. Evolution of P for the oscillatory $\alpha\omega$-dynamo model of Sect 6.4 for $C_\alpha = 0.75$. The symmetric solution ($P = +1$), which already exists, is unstable. Hence the stable antisymmetric one represents the final state

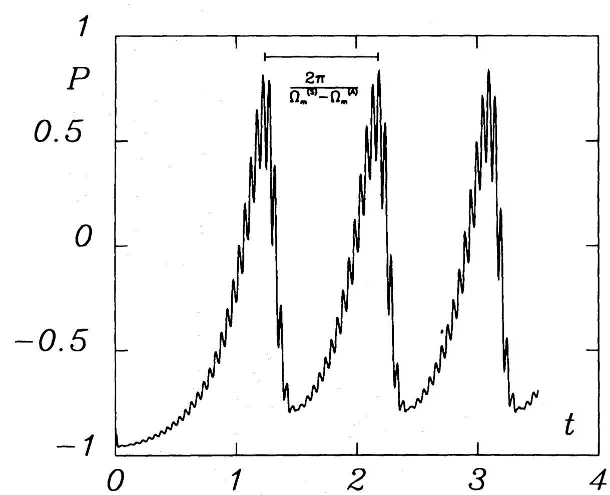

Fig. 10c. As Fig. 10b, but starting from $P = -0.9$. The same solution is reached from this initial condition too. The length of the bar in the upper part of the diagram is $2\pi/(\Omega_m^{(S)} - \Omega_m^{(A)})$, where $\Omega_m^{(S/A)}$ are the nonlinear frequencies for the pure solutions. This time coincides with the long term period

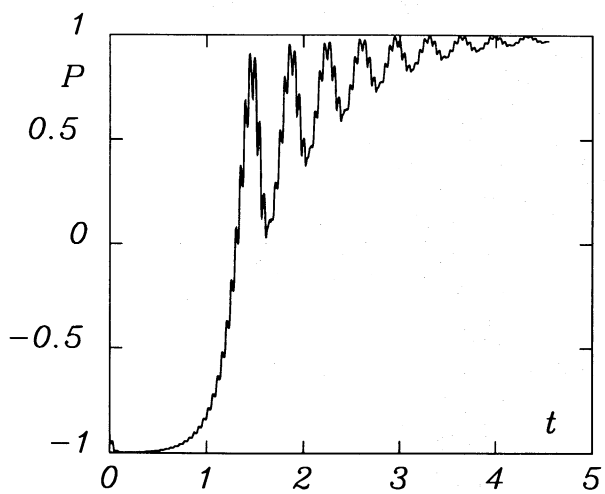

Fig. 10d. Same as Fig. 10a, but with $C_\alpha = 1.0$. Although the initial field is predominantly antisymmetric it evolves into the symmetric solution, thus showing its stability for this dynamo number

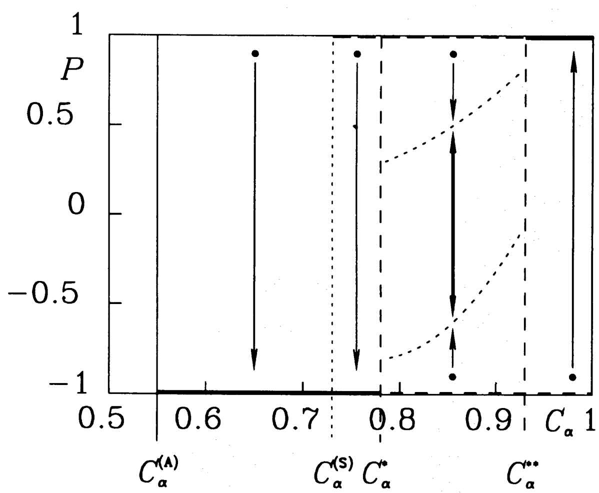

Fig. 10e. A sketch of the attractor scenario of the oscillatory $\alpha\omega$-dynamo model of Sect. 6.4. In contrast to the model discussed in Fig. 8e the antisymmetric solution loses stability before the symmetric one becomes stable. Hence there is a region $C_\alpha^* < C_\alpha < C_\alpha^{**}$ where no stable solution of pure parity exists. The solution varies between states of predominantly symmetric and antisymmetric appearance (see Fig. 10b)

solution is stable and obviously the final state for arbitrary initial conditions (Fig. 10d).

From these calculations we may conclude that there is a value C_α^* with the property that the antisymmetric solution is stable for $C_\alpha < C_\alpha^*$ and unstable for $C_\alpha > C_\alpha^*$. Furthermore there is a value $C_\alpha^{**} > C_\alpha^*$ such that the symmetric solution is unstable for $C_\alpha < C_\alpha^{**}$ but stable for $C_\alpha > C_\alpha^{**}$. For $C_\alpha^* < C_\alpha < C_\alpha^{**}$ no stable nonlinear solution of pure parity exists (Fig. 10b, c).

One is tempted to apply the main result of these investigtions to the Sun. It is well known that the poloidal field is not purely antisymmetric, e.g. it was observed that the polar caps reverse polarity at different times (e.g. Babcock, 1959), thus indicating a superposed symmetric (quadrupole) field. The field geometry

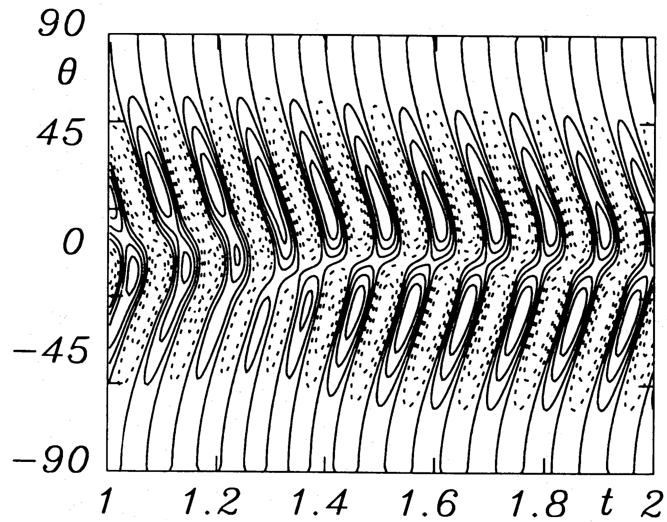

Fig. 10f. Butterfly diagram showing the toroidal field component at the level $r = 0.95$ in the $t-\theta$ plane for the model of Fig. 10b. The time interval, starting at $t = 1$ (see Fig. 10b), is a bit longer than a full period of parity variation. The nearly symmetric field on the left with $B_\phi \neq 0$ at the equator evolves into a antisymmetric one in the middle of the figure with $B_\phi \approx 0$ at the equator

calculated for $C_\alpha = 0.9$ shows similar features, the relative magnitude of antisymmetric and symmetric part slowly changing over the long period. However, in the case of the Sun, one must take into account that the butterfly diagram, which represents the toroidal field and so the strong part of the solar magnetic field, does not show significant deviations from antisymmetry. In addition, Stenflo and Vogel (1986) have not found even parity field parts of the poloidal field with a definite period.

The process of change of symmetry lasts for many periods, as can be seen from Fig. 10e showing the toroidal field at the depth $r = 0.95$ in the $t - \theta$ plane (butterfly diagram). One clearly sees that the mean magnetic field near the equator grows from (nearly) zero to a maximum, when the preferred symmetric configuration is reached.

7. Conclusions

We have shown that, for all considered dynamo models, the kinematic growth rates of fields of different parities are asymptotically equal as the dynamo numbers increase. Hence it is clear that a selection of a field with a certain parity cannot in general be explained by consideration of kinematic growth rates.

We then considered the behaviour of some models taking into account a nonlinear back-reaction of the magnetic field of various forms. In general we confirm the finding of Krause and Meinel (1988) that the stability of the nonlinear solutions provides the parity selection, although here, because more complicated models are considered, the phenomena are more complex. We confirmed that the first excited solution (in the order of growing dynamo number) is, for a certain range, the only stable one and that the higher solutions are at first unstable. However, in two cases it was found that there is a certain value C_α^* of the dynamo number, beyond which the second nonlinear solution becomes also stable (see Fig. 8e). The final state proves to be dependent on the initial conditions being, however, always of one symmetry. No mixture of fields with different symmetries appeared.

The higher bifurcation points are of less physical interest since the solutions will not be found or the corresponding fields observed because they are unstale. In contrast C_α^* is a quantity of interest since it characterizes the beginning of the range of the dynamo number where more than one stable nonlinear solution exists.

A new situation appears in our last example, where an oscillatory $\alpha\omega$-dynamo has been considered. For a constant C_ω and with increasing C_α the antisymmetric solution is at first stable. However, when C_α is increased more, it loses its stability, whilst the symmetric solution remains still unstable. No stable oscillating solution of a definite parity exists. Any initial field is attracted by a field with two periods: a long term oscillation between the unstable solutions of genuine symmetries superposed over the normal magnetic cycle. For even larger C_α the symmetric solution becomes stable. Obviously this model is worthy of further investigation.

The basic mechanism stabilizing or destabilizing different solutions is not well understood. To clarify this it therefore seems necessary to enlarge the sample of dynamo models with different stability behaviour. For example it would be important for application to the Sun to know under which conditions the oscillatory $A0$ mode is stable. Furthermore, the stability analysis of spherical dynamos has so far been restricted to axisymmetric analysis. So we do not know whether a solution, which is here proved to be stable, will respond similarly for non-axisymmetric disturbances. Results of Rädler and Wiedemann (1989) suggest that some of our solutions may possibly be unstable to non-axisymmetric perturbations.

Observations of the magnetic fields show more or less significant deviations from the basic symmetry, e.g. the inclination of the Earth's dipole or the sectorial structure of the Sun. Probably these deviations from symmetry have to be explained by models where the condition of exact symmetry of the internal structure and motions is relaxed from the beginning. This is, however, beyond the scope of this paper.

References

Babcock, H.D.: 1959, *Astrophys. J.* **130**, 364

Brandenburg, A., Moss, D., Tuominen, I.: 1989, *Geophys. Astrophys. Fluid Dyn.* (in press)

Krause, F., Meinel, R.: 1988, *Geophys. Astrophys. Fluid Dyn.* **43**, 95

Krause, F., Steenbeck, M.: 1967, *Z. Naturforsch.* **22a**, 671

Krause, F., Rädler, K.-H.: 1980, *Mean-Field Magnetohydrodynamics and Dynamo Theory*, Akademie-Verlag, Berlin

Rädler, K.-H.: 1984, *Astron. Nachr.* **305**, 289

Rädler, K.-H., Bräuer, H.J.: 1987, *Astron. Nachr.* **308**, 101

Rädler, K.-H., Wiedemann, E.: 1989, *Geophys. Astrophys. Fluid Dyn.* (in press)

Roberts, P.H.: 1972, *Phil. Trans. Roy. Soc.* **274**, 663

Proctor, M.R.E.: 1977, *J. Fluid Mech.* **80**, 769

Steenbeck, M., Krause, F.: 1969, *Astron. Nachr.* **291**, 49

Stenflo, J.O., Vogel, M.: 1986, *Nature* **319**, 285

Stix, M.: 1974, *Astron. Astrophys.* **37**, 121

Yoshimura, H., Wu, F., Wang, Z.: 1984, *Astrophys. J.* **280**, 865; **283**, 870; **285**, 325

Zeldovich, Ya.B., Ruzmaikin, A.A., Sokoloff, D.D.: 1983, *Magnetic fields in Astrophysics*, Gordon and Breach